Research Square

Preprints are preliminary reports that have not undergone peer review.
They should not be considered conclusive, used to inform clinical practice,
or referenced by the media as validated information.

Energy sensing OsSnRK1b and its regulator OsCTK1 promote chilling-induced stomatal closure and chilling tolerance in rice

Jian Hua

jh299@cornell.edu

Cornell University https://orcid.org/0000-0002-3777-3344

Jiawen Wu

Nanjing Agricultural University

Baohong Zou

Nanjing Agricultural University

Huimin Liu

Nanjing Agricultural University

Veronica Perez

Cornell University

Yao Zhang

College of Life Sciences, Northeast Agricultural University

Pavol Vadovic

Cornell University

Yuan Jiang

Cornell University

Shengsong Guo

University of Minnesota https://orcid.org/0009-0004-6185-1308

Rui Yang

Nanjing Agricultural University

Shiyan Liu

Nanjing Agricultural University

Shan Lu

Nanjing Agricultural University

Article

Keywords:

Posted Date: November 12th, 2025

DOI: https://doi.org/10.21203/rs.3.rs-7447278/v1

License: This work is licensed under a Creative Commons Attribution 4.0 International License.
Read Full License

Additional Declarations: There is **NO** Competing Interest.

Version of Record: A version of this preprint was published at Nature Communications on August 7th, 2026. See the published version at https://doi.org/10.1038/s41467-026-76376-9.

Abstract

Plants employ diverse physiological strategies for cold tolerance. Here we report an important role of low energy response and stomatal closure control in chilling tolerance through the study of SNF1-Related Kinase 1 (OsSnRK1) and its regulator Chilling Tolerance Kinase 1 (OsCTK1) in rice. OsSnRK1b, an isoform of OsSnRK1 alpha subunit, is found to have an evolutionarily conserved function in low energy response. It is positively regulated by OsCTK1 at the protein stability level through phosphorylation. Both OsCTK1 and OsSnRK1b promote chilling-induced stomatal closure and chilling tolerance, shown by slower stomatal closure and lower survival rate after chilling exposure in their respective loss of function mutants. Transcriptome analysis revealed that chilling induces low energy response which is largely dependent on OsSnRK1b. Overexpression of OsSnRK1b enhanced chilling induced stomatal closure response and promoted chilling tolerance in an OsCTK1-dependent manner. Furthermore, both OsCTK1 and OsSnRK1b promote expression of stress response gene Abscisic Acid Insensitive 5 (OsABI5) and inhibit accumulation of growth-associated ribosome protein OsRPS6 under chilling conditions. The function of CTK1 and SnRK1 in chilling tolerance, stomatal control, and growth inhibition are also observed in Arabidopsis and maize, indicating a conserved role of energy signaling in chilling tolerance and a contribution of stomatal aperture control to chilling tolerance in plants.

Introduction

Low-temperature stress poses a major challenge to plant growth and development and is a key factor limiting crop productivity and geographical distribution[1-3]. To cope with cold stress, plants employ a suite of physiological, biochemical and molecular adaptations, including changes in membrane lipid composition, accumulation of compatible solutes, activation of antioxidant systems to scavenge reactive oxygen species (ROS), and modulation of stress-responsive hormone levels[4,5]. Prior exposure to moderately low temperatures can enhance tolerance to extreme cold, a phenomenon termed cold acclimation[6-8]. Low temperature rapidly triggers calcium influx and ROS bursts, which serve as early signaling events to initiate transcriptional reprogramming. The CBF (C-repeat binding factor) transcription factors and their regulator ICE1 (Inducer of CBF expression) are key conserved players in cold signaling in diverse species including Arabidopsis, rice, and maize[9,10]. This cold-induced transcriptional response ultimately promotes expression of cold-responsive genes, leading to the accumulation of antifreeze proteins, osmoprotectants, and remodeling of the lipidome, processes essential for maintaining cellular homeostasis and enhancing low-temperature tolerance[2,11,12].

While molecular regulation of transcriptome change has been extensively studied for cold response in plants, broader physiological strategies at organismal level that contribute to cold tolerance are less well understood. Stomatal movement control is critical for adaptation to the environment, as it modulates gas exchange for photosynthesis and controls water loss for tolerance to drought and heat[13]. Stomatal movement has also been reported to occur in response to cold[14], and it was associated with cold-induced wilting and death in *Arabidopsis thaliana*, *Phaseolus vulgaris*, and *Nicotiana tabacum*[15-17].

Interestingly, multiple genes critical for cold acclimation, including *OST1* (*Open stomata 1*) and *CNGCs* (*Cyclic nucleotide-gated channels*), are important for cold induced stomatal closure. Notably, OST1, a regulator of ABA induced stomatal closure, can phosphorylate ICE1 to enhance CBF signaling pathway under cold stress[18-20]. The rice OsCNGC14/15/16 proteins that promote cold-induced stomatal closure are positive regulators of chilling tolerance[21]. These observations suggest a role for cold induced stomatal closure in cold tolerance.

Low energy response is a physiological response to energy depletion exemplified by starvation. A low energy status is also associated with some abiotic stresses including extended periods of salt and drought[3,22], but its association with cold stress has not been investigated. In yeasts and animals, SNF1-related kinase (SnRK1/AMPK) proteins function as low energy sensors and coordinate catabolic activation and anabolic repression to maintain cellular energy homeostasis[23]. They trigger rapid cellular adaptation under low energy stress through phosphorylating key metabolic enzymes and transcription factors, thereby reprograming transcriptional network and metabolism to promote catabolism and repress anabolism[23,24]. Plant SnRK1 is also critical for adaptation to energy-deficient conditions including extended darkness and hypoxia[25,26]. It is also shown to be important for tolerance to biotic and abiotic stresses[24,27,28]. SnRK1 consists of a catalytic α-subunit and regulatory β- and γ- subunits[29]. The α-subunit consists of a N-terminal Ser/Thr kinase domain and a C-terminal regulatory domain that mediates its interaction with the β- and γ- subunits[30]. In Arabidopsis, three genes (*KIN10*, *KIN11* and *KIN12*) encode the α-subunit of SnRK1 (SnRK1α). Among these, the KIN10 subunit translocates to the nucleus to de-repress metabolic stress-responsive genes under darkness, inhibited photosynthesis, or hypoxia[31]. It phosphorylates transcription factors bZIP63 and bZIP53 for starch synthesis and proline metabolism during dark-induced low-energy stress, respectively[32,33]. In rice, four isoforms of SnRK1α could be identified by sequence homology and they are named OsSnRK1a, OsSnRK1b, OsSnRK1c and OsSnRK1d (https://www.ricedata.cn/). OsSnRK1a is shown to regulate starvation response by promoting starvation-responsive genes under energy limitation but repressing these genes under energy-sufficient conditions through its interaction with the H3K27me2/3 demethylase JMJ705[34]. Whether a low energy response pathway is involved in cold tolerance remains unknown in plants. *OsCTK1* (*Chilling tolerance kinase 1*) is a positive regulator of chilling tolerance in rice as evidenced by a lower survival rate under chilling in its loss of function (LOF) mutants compared to the wild type[35]. Natural variation of the *OsCTK1* gene is a major contributor to chilling tolerance variation in *Indica* rice. The CT (Chilling tolerant) variant of *OsCTK1*, with a four amino acids insertion, exhibits a higher kinase activity and confers a greater chilling tolerance compared to the CS (Chilling sensitive) variant[35]. OsCTK1 belongs to a serine/threonine kinase family CKI (Casein kinase I) which has a broad regulatory function[36,37,38,39,40]. The Arabidopsis OsCTK1 homologous proteins, CK1.3 and CK1.4, are shown to regulate blue light signaling by phosphorylating the cryptochrome receptor CRY2 (Cryptochrome 2)[39]. OsCTK1 may target multiple phosphorylation substrates for its function, including OsP3B (Acidic ribosomal protein 3B), OsCNGC9, and OsMKP1 (Mitogen-activated protein kinase phosphatase 1)[35].

In this study, we further investigated the regulatory mechanism of chilling tolerance through the study of another substrate of OsCTK1, OsSnRK1b. We found that OsSnRK1b, like OsSnRK1a, is also a low energy sensing kinase. OsCTK1 phosphorylates and stabilizes the OsSnRK1b. Similar to *OsCTK1*, *OsSnRK1b* promotes stomatal closure in response to chilling and enhances chilling tolerance. They both regulate the chilling-induced expression of stress-induced genes and repress the accumulation of the growth associated proteins. These findings indicate that energy metabolism and stomatal regulation are critical mechanisms for chilling tolerance in rice.

Results

OsCTK1 positively regulates stomatal closure in response to chilling

In addition to a lower survival rate and a higher ion leakage after chilling [35], the *Osctk1-2* and *Osctk1-3* LOF mutants had a rapid leaf-drooping phenotype after chilling treatment when compared to the wild type Nipponbare (NIP) (Fig. 1A). The *Osctk1* mutants also had a faster water loss and a more rapid leaf curling after chilling exposure compared to the wild type (Fig. 1B and Supplementary Fig. 1A-B). These defects promoted us to measure stomatal aperture in the *Osctk1* mutant after chilling treatment. Stomatal closing was observed in the wild-type plants at 1 h and continued at 3 h and 9 h, but it was not observed till 3 h in *Osctk1-3* and9 h in *Osctk1-2* (Fig. 1C-D). In addition, both mutants had a larger stomatal aperture at all time points measured compared to the wild type (Fig. 1C-D). This stomatal defect was supported by thermal imaging where a lower leaf temperature was detected in the *Osctk1* mutants compared to the wild type (Fig. 1E). This is corroborated with a higher transpiration rate in the mutants than the wild type under normal and chilling conditions (Fig. 1F). The *OsCTK1* gene is expressed in guard cells, as shown by positive signal of *β*-Glucuronidase (GUS) reporter in transgenic plants carrying the GUS reporter gene under the control of the *OsCTK1* promoter (Supplementary Fig. 1C). This indicates an expression of *OsCTK1* in guard cells and suggests a cell-autonomous function of *OsCTK1* in guard cells.

The activity of *OsCTK1* in promoting stomatal closure is aligned with its activity in promoting survival rate under cold as shown by its two natural variants. The CT variant of *OsCTK1* was previously shown to confer a higher survival rate under chilling stress than the CS variant[35]. Transgenic *Osctk1-2* lines carrying the CT variant had a wild-type phenotype while lines carrying the CS variant partially complemented the *Osctk1-2* mutant, as shown by reduced stomatal aperture and transpiration rate after a 6°C chilling treatment (Supplementary Fig. 1D-I). Therefore, the function of OsCTK1 in stomatal closure control is highly correlated with its function in promoting survival under chilling.

OsCTK1 phosphorylates OsSnRK1b

We conducted *in vitro* phosphoproteomics to identify phosphorylation targets of OsCTK1 that might mediate the function of OsCTK1 in stomatal movement control. OsSnRK1b and OsSnRK1c were among the Mass Spec identified candidate target proteins as a shared peptide of these two proteins were

identified as phosphorylated by the recombinant OsCTK1. We chose these two proteins for further study because theirArabidopsis homolog KIN10 was previously implicated in stomatal movement control under normal growth temperature[41] (Supplementary Fig. 2A).

OsSnRK1b was selected among the two proteins for assaying the interaction OsCTK1, as 1b and 1c are highly homologous. Direct physical interaction between OsCTK1 and OsSnRK1b was verified in planta and *in vitro* by Co-Immunoprecipitation (Co-IP) assays (Supplementary Fig. 2B). A direct phosphorylation of OsSnRK1b by OsCTK1 was observed by an *in vitro* kinase assay (Fig. 2A). The recombinant His-OsSnRK1b protein had an autophosphorylation activity, but the addition of GST-OsCTK1 in the kinase reaction resulted in a stronger phosphorylation of His-OsSnRK1b protein (Fig. 2A). In addition, natural variants of OsCTK1 exhibited a differential phosphorylation activity on OsSnRK1b in the *in vitro* kinase assay. The CT variant of OsCTK1 exhibited a higher phosphorylation on OsSnRK1b than the CS variant, and the critical Indel polymorphism also altered the phosphorylation level of the CT and the CS variants (Supplementary Fig. 2C).

Phosphorylation of OsSnRK1b that is dependent on OsCTK1 was also detected in protoplast cells expressing a GFP-tagged OsSnRK1b by phos-tag gels. A slower migrating band of GFP-OsSnRK1b was observed in the wild type cells but not in the *Osctk1-2* mutant cells (Fig. 2B). This differential band pattern was also observed from protoplast cells incubated further at 6°C for 1 h. Treatment of protein extracts by calf intestine phosphatase (CIP) abolished this slow migrating band, indicating that it was indeed a phosphorylated form of OsSnRK1b-GFP.

We identified three residues, Thr^{173}, Ser^{174} and Ser^{347}, as potential phosphorylation sites of OsCTK1 in OsSnRK1b through two approaches. Above mentioned *in vitro* phosphoproteomics detected phosphorylation of Thr^{173} and/or Ser^{174}. MassSpec analysis of GFP tagged OsSnRK1b expressed in protoplast cells revealed Ser^{347} phosphorylation in the wild-type but not the *Osctk1-2* mutant protoplast cells (Supplementary Fig. 2D). Mutating Thr^{173} and Ser^{174} of SnRK1b to Ala resulted in a 20% decrease in phosphorylation of OsSnRK1 (Supplementary Fig. 2E), while an 89% reduction of phosphorylation was observed when mutating Ser^{347}, Thr^{173} and Ser^{174} of OsSnRK1bsimultaneously to Ala *in vitro* kinase assay with OsCTK1 (Fig. 2A). As autophosphorylation accounted for about 29% phosphorylation in the wild-type OsSnRK1b, this indicates an 85% reduction (11% versus 71%) of phosphorylation of OsSnRK1b by OsCTK1 from mutations of these three residues (Fig. 2A).

OsCTK1 stabilizes OsSnRK1b through phosphorylation

OsCTK1 was found to affect the abundance of OsSnRK1b when OsSnRK1b protein was detected by an antibody that targets OsSnRK1 members (Fig. 2C). This antibody primarily detects OsSnRK1b, because a similar reduction (71% and 73%) of the signal compared to the wild type was observed in the *Ossnrk1b1c* double mutant and a *Ossnrk1b* single mutant (as described in the next result section) (Fig. 2C). Strikingly, the *Osctk1-2* mutant had a 46% reduction of OsSnRK1 proteins detected by this antibody compared to the wild type (Fig. 2C). This reduction of OsSnRK1 protein abundance was not due to a reduced RNA

transcript of *OsSnRK1* in the *Osctk1-2* mutant (Supplementary Fig. 2F), indicating an effect on OsSnRK1b at the protein level by OsCTK1. A cell-free protein degradation assay indicates that a lower protein stability contributes to the low abundance of OsSnRK1b in the *Osctk1-2* mutant. The recombinant His-OsSnRK1b protein had a faster degradation when incubated with protein extracts from *Osctk1-2* mutant than from those of the wild type (Fig. 2D).

The stability of OsSnRK1b was affected by its OsCTK1 phosphorylation sites. The His tagged mutant OsSnRK1b protein with three phosphorylation site mutation to Ala, His-OsSnRK1b$^{TSS\text{-}AAA}$, had a faster degradation compared to the wild-type His-OsSnRK1b form when incubated with protein extracts from wild-type plants (Fig. 2D). In contrast, when incubated with protein extracts from the *Osctk1-2* mutant, the His-OsSnRK1b$^{TSS\text{-}AAA}$ protein had a degradation rate similar to the wild-type His-OsSnRK1b (Fig. 2D). These findings suggest that phosphorylation of OsSnRK1b at these sites affect the protein stability in an OsCTK1-dependent manner.

OsCTK1 affects the subcellular localization of OsSnRK1b in addition to its protein abundance. When expressed in protoplast cells, the GFP-OsSnRK1b fusion protein had both nuclear and cytosol distributions as assayed by nuclear fractionation. It has a lower nuclear accumulation and a higher cytosol accumulation in the *Osctk1-2*mutant cells compared to the wild type (Fig. 2E). The nuclear/cytosol distribution of OsSnRK1b was likely affected by the three OsCTK1 phosphorylation residues. A lower nuclear accumulation and a higher cytosol accumulation was observed for GFP-OsSnRK1b$^{TSS\text{-}AAA}$ protein compared to the GFP-OsSnRK1b protein when expressed in wild-type protoplasts (Fig. 2F). These data suggests that phosphorylation of OsSnRK1b by OsCTK1 may enhance its translocation to the nucleus.

OsSnRK1b promotes stomatal closure and survival under chilling

The function of *OsSnRK1b* and *OsSnRK1c* was analyzed through the mutants generated by CRISPR/Cas9 gene editing. Four LOF *OsSnRK1b* mutant lines were obtained, with the *-1* and *-2* alleles independently created from the *-3* and *-4* alleles from different pairs of RNA targets (Supplementary Table 1). The *Ossnrk1b1c* mutant was an *Ossnrk1b Ossnrk1c* double mutant as it contained an additional mutation in the *OsSnRK1c* gene (Supplementary Table 1). All four mutant lines exhibited a similar phenotype in the initial characterization, and therefore *Ossnrk1b1c* double mutants and *Ossnrk1b-3* (*Ossnrk1b* single mutant) were used for further analysis.

Both *Ossnrk1b1c* and*Ossnrk1b-3* exhibited more chilling susceptibility compared to the wild-type NIP plant. After 6°C treatment, leaf rolling and leaf drooping occurred much earlier in the mutants than the wild type (Fig. 3A, Supplementary Fig. 3A). These mutants also had a similar faster water loss, slower stomatal closure, and higher transpiration than the wild type (Fig. 3B-E, Supplementary Fig. 3B). The other two alleles, *Ossnrk1b-1* and*Ossnrk1b-4*, exhibited the same stomatal closure and water retention defects as the *Ossnrk1b1c* and*Ossnrk1b-3* alleles (Supplementary Fig. 3C-F). These data indicate that the loss of *OsSnRK1b* function compromised chilling-induced stomatal closure.

The *Ossnrk1b* mutants also showed more susceptibility to chilling compared to the wild type as measured by leaf damage and survival rate (Fig. 3F). They had a higher ion leakage to a similar degree in leaf tissues after 24 h of chilling treatment compared to the wild type (Fig. 3G). The survival rates from 2 d of 6℃ treatment were 28% and 20% for the two mutants, lower than the rate of 58% for the wild type (Fig. 3H and Supplementary Fig. 3G-H). These data indicate that the loss of *OsSnRK1b* function leads to reduced chilling tolerance. The *Ossnrk1b Ossnrk1c* double and *Ossnrk1b-3* single mutants exhibited a similar degree of defects under chilling. This indicates that the *OsSnRK1c* gene had no detectable function in chilling tolerance in the absence of the *OsSnRK1b* function. These data indicate that the *OsSnRK1b* plays a dominant role over *OsSnRK1c* or an equal role as the *OsSnRK1c* isoform in chilling responses (Fig. 3A-H). The relative function of *OsSnRK1b* and *OsSnRK1c* isoforms could be further verified when single mutants of the *OsSnRK1c* form become available.

Overexpressing *OsSnRK1b* promotes chilling tolerance and chilling induced stomatal closure in an *OsCTK1*-dependent manner

To further analyze the function of OsSnRK1b and its regulation by OsCTK1, we analyzed transgenic lines overexpressing *OsSnRK1b* in wild-type NIP (named OE-*OsSnRK1b*/NIP) and *Osctk1-2* (named OE-*OsSnRK1b*/*ctk1*), respectively. Consistent with findings *in vitro*, the GFP-OsSnRK1b protein had a lower accumulation in the two OE-*OsSnRK1b*/*ctk1* lines compared to the two OE-*OsSnRK1b*/NIP lines, despite comparable *OsSnRK1b* RNA expression in these four lines (Supplementary Fig. 3I-J). When transgenic plants were subject to chilling, GFP-OsSnRK1b has a more pronounced reduction in *Osctk1-2* lines compared to the wild type lines (Supplementary Fig. 3J).

Overexpression of *OsSnRK1b* was found to promote stomatal closure and enhance chilling tolerance in the wild type. After 6°C chilling treatment, the two OE-*OsSnRK1b*/NIP lines showed delayed leaf rolling and drooping compared to the wild type (Fig. 3I). Water loss was lower at 3 h and 9 h of chilling treatment in the overexpression lines compared to the wild type (Supplementary Fig. 3K). The overexpression lines also had smaller stomatal apertures at 28°C and faster stomatal closure upon 6°C exposure (Supplementary Fig. 3L), resulting in higher leaf temperature and lower transpiration rate both before and after chilling compared to the wild type (Fig. 3J-K). In addition, the OE-*OsSnRK1b*/NIP transgenic lines suffered less chilling damage, as shown by lower ion leakage at 24 h (Fig. 3L-M) and higher survival rates (Fig. 3N) after 3.5 days at 6°C. Together, these data indicate that overexpression of *OsSnRK1b* promotes stomatal closure and confers a higher chilling tolerance.

The enhanced chilling tolerance and stomatal closure by *OsSnRK1b* overexpression was not observed in the *Osctk1-2* mutant background (Fig. 3I). The two OE-*OsSnRK1b*/*ctk1* lines behaved the same as the *Osctk1-2* mutant plant before and after chilling treatment, including earlier leaf dropping, higher water loss, more open stomata, and higher transpiration rate compared to the wild type (Fig. 3I-K and Supplementary Fig. 3K-L). The OE-*OsSnRK1b*/*ctk1* lines also had higher ion leakage (Fig. 3M) and lower survival rate (Fig. 3N) compared to the wild type. These data indicate that the effects of *OsSnRK1b* overexpression on chilling tolerance and stomatal aperture are dependent on OsCTK1.

OsSnRK1b is required for starvation response

Because AtSnRK1α in Arabidopsis and OsSnRK1a in rice are shown to be low energy sensing kinases [23,34], we assessed whether OsSnRK1b is also involved in low energy response. The *Ossnrk1b* mutantsandthe OE-*OsSnRK1b* lines were subject to starvation with continuous darkness for 7 days (Fig. 4A). Both the *Ossnrk1b1c* and the *Ossnrk1b-3* mutants exhibited a larger bleached area compared to the wild type, corroborated by reduced chlorophyll levels in leaves, compared to the wild type (Fig. 4B-C). The bleaching and chlorophyll loss in the *Ossnrk1b* mutants was to a similar extent as the *Ossnrk1a-1* mutant (Supplementary Fig. 4A-D). Conversely, the OE-*OsSnRK1b* lines exhibited a reduced bleached area and higher chlorophyll levels than the wild type (Fig. 4A-C). This indicates that OsSnRK1b has a conserved role in low energy stress response. In addition, the *Ossnrk1a-1* mutant [42] (Supplementary Fig. 4A) which was shown to be defective in low energy response, had a significantly lower survival rate and higher transpiration rate than the wild-type after chilling treatment (Supplementary Fig. 4E-G), indicating that OsSnRK1a has a similar function to OsSnRK1b in chilling tolerance.

OsSnRK1b is required for chilling induced growth inhibition

We hypothesize that low energy response contributes to chilling response in plants because SnRK1b and SnRK1a are both important for low energy tolerance and chilling tolerance. To test this, we examined transcriptomic response to chilling in the wild type and the *Ossnrk1b* mutants by RNA sequencing (RNA-seq) analysis. The wild-type plant had 1478 cold (6℃ for 3 h) induced DEGs, and 849 (57%) of them were also induced by starvation based on a previous report (Wang et al 2021) (Fig. 4D), suggesting a contribution of low energy response to transcriptome reprogramming under chilling. The *Ossnrk1b* mutants had a reduced number of cold-induced genes (959) compared to the wild type, and a smaller proportion (163, 16.3%) of these genes overlapped with chilling induced and starvation induced genes compared to the wild type (Fig. 4E-F). Therefore, about half (51%) of cold-induced DEGs and 81% of the cold-induced starvation-responsive genes are dependent on *OsSnRK1b* (Fig. 4E-F), suggesting an important role of *OsSnRK1b* in inducing starvation response genes under cold.

As low energy response balances plant growth and stress responses, we further investigated the regulation of growth process under chilling by *OsSnRK1b* and *OsCTK1*. The phosphorylation of Ser^{240} of the ribosome protein RPS6 (a marker for TOR regulated growth) and the abundance of RPS6 (an indicator of growth) were analyzed in the mutants before and after chilling stress treatment (Fig. 4G). Strikingly, both the *Ossnrk1b1c* and the *Osctk1-2* mutants had a higher amount of Ser^{240} phosphorylation in OsRPS6 compared to the wild type at 28℃. The difference became more pronounced after chilling treatment (Fig. 4G). The wild type had a reduced Ser^{240} phosphorylation at 3 h and 12 h after chilling, reflecting the inhibition of growth at early phase of chilling stress response, but the *Osctk1-2* and *Ossnrk1b1c* mutants had increased phosphorylation after chilling (Fig. 4G), suggesting a loss of growth inhibition under chilling. Similarly, the OsRPS6 protein amount was at a higher level in these two mutants compared to the wild type under 28℃ growth condition. In addition, the RPS6 amount decreased at 3 h, recovered at 12 h in the wild type, but it did not decrease after chilling and remained the same amount

throughout the chilling treatment in the two mutants (Fig. 4H). These findings suggest that *OsSnRK1b* and *OsCTK1* inhibit growth processes in general and more so under chilling stress.

OsSnRK1b and *OsCTK1* regulate chilling-induction of the stress response gene *OsABI5*

Because OsSnRK1b regulates stomatal closure which is known to be associated with the ABA response pathway, we asked whether it regulates the ABA stress response pathway under cold. Chilling induced 74 'ABA-responsive genes' (GO:0009737) among the 495 genes under this GO term, which was not significantly enriched among the chilling induced DEGs in the wild type. Nevertheless, 43 of them were not induced by chilling in the *Ossnrk1b1c* mutant, indicating a dependence on *OsSnRK1b* for chilling induction. We subsequently investigated the expression of *OsABI5* that encodes a major transcription factor for ABA response. qRT-PCR revealed that *OsABI5* expression was induced by 6°C treatment at 3 h or 24 h in the wild type but not in the *Ossnrk1b1c* mutants (Fig. 5A). *OsCTK1* was also found to regulate the RNA expression of *OsABI5*. Despite having a higher expression of *OsABI5* compared to the wild type at 28°C, the *Osctk1-2* mutant plants had no induction of *OsABI5* gene expression by chilling and a lower *OsABI5* expression compared to the wild type under chilling (Fig. 5B).

The regulation of *OsABI5* by *OsSnRK1b* was also seen in the OE-*OsSnRK1b* transgenic plants. The expression of *OsABI5* was higher in the OE-*OsSnRK1b* transgenic plants than in the wild type, but it was the same in the OE-*OsSnRK1b*/*ctk1* lines as in the *Osctk1-2* mutant(Fig. 5C). These results indicated that *OsSnRK1b* and *OsCTK1* are both required for the induction of *OsABI5* in response to chilling, and *OsCTK1* has an additional role in repressing *OsABI5* expression under non-stress conditions.

OsABI5 positively regulates chilling tolerance and stomatal closure

A previous study shows that an *Osabi5* mutant had reduced germination and seedling survival under cold compared to the wild type plants[62]. To further investigate the role of OsABI5 in the cold stress response, we analyzed two independent LOF mutants of *OsABI5*, *Osabi5-1* and *Osabi5-2*, generated by CRISPR/Cas9 gene editing in the ZH11 background (Supplementary Table 1). Both *Osabi5* mutants exhibited more extensive leaf drooping compared to the wild-type parent ZH11 after a 6℃ treatment (Fig. 5D). They also had higher ion leakage (Fig. 5E) and lower survival rates (Fig. 5F) compared to the wild type. In addition, the *Osabi5* mutants had a higher water loss after chilling compared to the wild type (Fig. 5G and Supplementary Fig. 5A-B).

The chilling susceptible defect in the *Osabi5* mutants was accompanied by a larger stomatal aperture in the mutant than the wild type after chilling (Fig. 5H). This stomatal aperture defect is not chilling specific, as the *Osabi5* mutants had a larger aperture without chilling treatment as well. In addition, the mutants closed stomata in response to chilling a similar dynamic to the wild type (Fig. 5H). Correlated with stomatal aperture defect, the *Osabi5* mutants had a higher transpiration rate before and after chilling treatment compared to the wild type, and its leaf surface temperature was lower than the wild type at 3 h after 6°C treatment (Supplementary Fig. 5C-D). These results indicate that *OsABI5* promotes stomatal closure in general, but it does not significantly affect the chilling induction of stomatal closure.

OsCTK1 and *OsSnRK1b* do not significantly affect the expression of *CBF* related genes under chilling

We also investigated whether *OsCTK1* and *OsSnRK1b* regulate expression of the *C-repeat binding factor* (*CBF*) or *dehydration-responsive element-binding* (*DREB*) genes. In the wild-type plants, chilling treatment at 6°C induced the expression of eight out of the nine *OsDREB* genes at both 3 h and 24 h (Fig. 5I-J). All eight genes were also induced by chilling in the *Ossnrk1b* mutants. However, the induction of *OsDREB* genes in *Ossnrk1b* mutants were significantly lower than in the wild type at 3 h, while most *OsDREB* genes showed no significant difference at 24 h (Fig. 5I). In contrast, the *Osctk1* mutant exhibited higher basal expression levels of seven *OsDREB* genes at normal growth temperature. After 24 h of 6°C treatment, the expression levels of these eight genes in the *Osctk1* mutant were not significantly different from those in the wild type (Fig. 5J). These findings indicate that OsCTK1 is not a positive regulator of *OsDREB* expression, and its role in chilling tolerance is likely independent of the CBF pathway. Although OsSnRK1b exerts minor effects on the expression of certain *OsDREB* genes, whether its function in chilling tolerance is primarily mediated through the CBF pathway remains to be elucidated.

Arabidopsis *SnRK1* and *CTK1* are regulators of chilling tolerance and chilling induced stomatal closure

To determine whether or not the involvement of low energy response in chilling tolerance is conserved in plants, we analyzed homologous genes of *SnRK1b* and *CTK1* in Arabidopsis. *KIN10* (At3g10190), an apparent ortholog of three *OsSnRK1* (*a, b,* and *c*) genes in rice (Supplementary Fig. 1A),has been shown to participate in starvation response [23]. The LOF *kin10* mutant exhibited a slower stomatal closure in response to chilling. When seedlings were exposed to 6°C, stomatal closing was observed as early as 3 h of treatment in the wild type, but no closing was observed even at 24 h of chilling treatment in the *kin10* mutant (Fig. 6A). Corroborated with the stomatal behavior, the *kin10* mutants had a higher transpiration rate compared to the wild type throughout the 24 h of 6°C treatment (Fig. 6B-C). It was also more susceptible to freezing, as evident by the reduced survival rate following a 5 h of -8ºC treatment compared to wild-type (Fig. 6D). Most strikingly, the *kin10* mutant exhibited a higher amount of growth associated molecular markers under chilling similarly to the *Ossnrk1b* mutant. Chilling treatment of 24 h reduced total RPS6 abundance and Ser^{240} phosphorylation in wild type, and the *kin10* mutant had a higher level of both total RPS6 and phosphorylation at $Ser^{240/244}$ compared to the wild type under both normal and chilling growth conditions (Fig. 6F).

The closest homolog of *OsCTK1* in Arabidopsis, *AtCK1.3*, was also found to play a role in chilling tolerance. Compared to the wild type, the *Atck1.3* mutant had a larger stomatal aperture under normal growth conditions as well as a delayed stomatal closure and increased transpiration rates throughout the 24 h period of chilling treatment (Fig. 6A-C). This mutant also had a reduced survival rate after 3 h of exposure to -8°C freezing stress compared to the wild type (Fig. 6E). In addition, the *Atck1.3* mutant had a higher RPS6 phosphorylation and accumulation than the wild type after 24 h of 6°C treatment (Fig. 6G).

The *ABI5* gene in Arabidopsis also promotes stomatal closure under both normal and low temperatures. The *Atabi5* mutant had a larger stomatal aperture and a higher transpiration rate under normal growth conditions (Fig 6A-C). Although it responded to chilling by closing the stomata in a similar dynamic as the wild type, the mutant had a larger stomatal aperture and a higher transpiration rate throughout 36 h chilling treatment (Fig 6A-C).

Maize *CTK1* is a positive regulator of chilling tolerance

We further investigated the function of the closest homolog of *OsCTK1* in maize, *ZmCTK1* (GRMZM2G156035). A LOF mutant of *ZmCTK1* gene was generated by CRISPR/Cas9, and this *Zmctk1-1* mutant was assayed for survival rates and stomatal closure response after chilling treatment. The wild-type maize plants exhibited stomatal closure after 1 h of 6ºC chilling treatment (Fig. 6H). While the *Zmctk1* mutant had a wild-type stomatal aperture under normal growth, it displayed a reduced stomatal closure upon 6ºC treatment compared to the wild type (Fig. 6H). Additionally, the *Zmctk1* mutant had a reduced survival rate (20%) than the wild type (61%) following a 3-week chilling treatment at 10ºC (Fig. 6I).

Similar to the rice *Osctk1* mutant, the maize *Zmctk1* mutant did not exhibit chilling induced growth marker inhibition. Chilling stress caused a reduction in total RPS6 abundance and a reduction of Ser^{240} phosphorylation in wild-type maize plant (Fig. 6J). The *ZmCTK1* mutant had a higher level of RPS6 and phosphorylated form of RPS6 with or without 1 day of chilling treatment (Fig. 6J). These findings indicate that *ZmCTK1* regulates chilling tolerance, chilling induced stomatal closure, and chilling induced RPS6 reduction.

Discussion

This study uncovers a new mechanism of chilling tolerance that involves low energy response for inhibiting growth and promote stress response under cold (Fig. 6K). The rice *OsSnRK1b* gene has an evolutionarily conserved function in starvation response, and it is also a positive regulator of chilling tolerance, as demonstrated by the altered starvation response and chilling responses in its LOF mutants and overexpression lines (Fig. 3F-H and L-N). In addition, induction of low energy responsive genes, largely carried out by *OsSnRK1b*, is part of transcriptome reprogramming in response to cold as revealed by RNA-seq analysis (Fig. 4D-F). Furthermore, *OsSnRK1b* is responsible for inhibiting growth and promoting stress response under cold, as indicated by the elevated growth status marker (OsRPS6 protein phosphorylation) and reduced expression of *OsABI5* under cold in the *Ossnrk1b* mutant (Fig. 4G-H and 5A-C). Together, these data indicate that low energy response is critical for chilling response and chilling tolerance. While the key low energy response regulator SnRK1α activates catabolism and represses anabolism to maintain cellular energy homeostasis under starvation stress, it inhibits growth and activates stress response under chilling stress. This mechanism is likely evolutionarily conserved among plants shown by a similar role for the *SnRK1α* genes in Arabidopsis and maize.

This study also identifies *OsCTK1* as a positive regulator of *OsSnRK1b*. The OsCTK1 protein phosphorylates and stabilizes the OsSnRK1b protein under both non-chilling and chilling conditions, as evidenced by the reduced protein abundance and nuclear accumulation of OsSnRK1b in the *Osctk1* mutant (Fig. 2C-F). This regulation is also supported by a similar LOF and overexpression effects of these two genes in chilling tolerance and chilling induced stomatal movement as well as the loss of *OsSnRK1b* overexpression effect in the absence of the *OsCTK1*. The direct involvement of starvation response for *OsCTK1* is yet to be tested, but this is suggested by the elevated RPS6 phosphorylation in the *Osctk1* mutant (Fig. 5H). Previous study identified a direct phosphorylation of SnRK1 by SnAK1/2 (SnRK1-activating kinases) at Thr-175 or Thr-176 residues that promotes the SnRK1α kinase activity in Arabidopsis[43,44]. These sites are distinct from the potential phosphorylation sites of OsSnRK1 by OsCTK1, suggesting different effects of these two regulators on OsSnRK1*α*. Besides the effect on the protein stability of OsSnRK1b, the effects of phosphorylation by OsCTK1 on the kinase activity of OsSnRK1b has not been determined (Fig. 2D), although its effect on nuclear localization of OsSnRK1b suggests a regulation of its activity as well (Fig. 2E-F).

SnRK1 was previously shown to regulate response to a number of abiotic stresses that induce low-energy status[23]. Drought stress induces stomatal closure and therefore limits CO_2 intake and ATP synthesis[45,46]. Salt stress, including Na^+ toxicity, disrupts thylakoid membrane integrity and inhibits photosynthesis system and ATP production[47]. Hypoxia induces transition from aerobic to anaerobic respiration, causing a decline in ATP yield[48,49]. Heat stress inactivates Rubisco activate, damages chloroplast structure, and impedes photosynthesis[50]. Low temperature may also induce low energy status, like starvation, drought, salt, hypoxia, and heat. Chilling stress is known to disrupt thylakoid membrane structure, inhibit chlorophyll synthesis, and inhibit electron transport chain. It also causes phase transition of membrane lipids from the liquid crystalline state to the gel state, leading to ion leakage. The involvement of SnRK1 in chilling tolerance suggests that low energy sensing pathway could have a broad function in stress tolerance. This conserved pathway may direct the physiological reprogramming for environmental adaptation. Under chilling stress, OsSnRK1b mediates the induction of stress-responsive genes (such as *OsABI5*) and suppression of growth-related markers (OsRPS6) (Fig. 6K), suggesting a coordination of stress and growth processes according to the environment. This coordination is likely not through the regulation of *DREB*/*CBF* expression, as the expression of *OsDREB* genes under chilling did not have reduced expression in the *Osctk1* and *Ossnrk1b* mutants compared to the wild type (Fig. 5I-J). Interestingly, the *Osctk1* and *Ossnrk1b* mutants accumulate higher amount of growth marker protein RPS6 under non-chilling condition, but these mutants did not exhibit increased growth compared to the wild type (Fig. 4G-H). This suggests a broad role of *OsSnRK1b* and *OsCTK1* genes in growth regulation other than the RPS6 associated pathway.

This study also highlights that stomatal aperture regulation as a critical physiological response in chilling tolerance. *OsCTK1* and *OsSnRK1b* both promote stomatal closure in response to chilling as well as survival under cold (Figs. 1A-F and 3A-N). *OsABI5*, a regulator of stomatal aperture regardless of chilling conditions, is also a positive regulator of chilling tolerance (Fig. 5D-H). Together with *OsCNGCs* in

rice and *OST1* in Arabidopsis, dual-function in stomatal closure and chilling tolerance for these genes strongly implicate stomatal movement control is an important part of chilling tolerance mechanism[18-21]. How *SnRK1* genes in rice and Arabidopsis regulate stomatal movement under chilling still awaits further investigation. *OsABI5* is a potential regulatory target, not necessarily a direct kinase target, as chilling induction of its transcript is reduced in the *OsSnRK1b* mutants. In addition, energy status markers such as sugar accumulation could affect stomatal movement, as starch degradation and glucose accumulation in guard cells could lead to stomatal opening[51,52]. Indeed, *KIN10* (*AtSnRK1*) overexpression was shown to promote light-induced starch degradation and thus stomatal opening[31].

This study shows that some *SnRK1α* members, *OsSnRK1b* in rice and *KIN10* in Arabidopsis, regulate low-temperature response and low energy response. It is not yet known whether all members of the *SnRK1α* family have dual functions. *KIN10* and *KIN11* in Arabidopsis were shown to be low energy sensors (in starvation response) while the role of *KIN12* in starvation response has not been tested[23]. *KIN10* is a positive regulator of chilling tolerance, but the function of the other two Arabidopsis genes in chilling tolerance are yet to be determined. Among the four members in rice, *OsSnRK1a* and *OsSnRK1b* each have dual function in starvation response and chilling tolerance. The function of *OsSnRK1c* and *1d* in chilling tolerance are yet to be determined by their LOF mutants. Whether or not a member has a more pronounced role in a specific stress response than other members is yet to be investigated in plants. Deciphering the shared or distinct functions of SnRK1 members in multiple stresses will provide insights into the evolution of these conserved proteins.

In conclusion, this study demonstrates the involvement of low energy response in chilling tolerance and supports stomatal closure control as a critical mechanism for chilling tolerance. The knowledge of chilling tolerance at the whole plant physiology level will facilitate the development of strategies for enhancing plant resilience in a changing environment.

Methods

Plant materials and growth conditions

The genetic backgrounds of rice mutant and transgenic plants in this study were ‘Nip’ or ‘ZH11’ as specified. Freshly harvested seeds were treated at 42℃ for a minimum of 14 days to break dormancy. Seeds were then soaked in water at room temperature for 3 to 5 days for germination. For hydroponic growth, germinated seeds with a similar development stage were transferred to a 96-well plate (with its bottom cut) that sits in water, as described previously[53]. Seedlings were grown in controlled chambers with 16 h of light and 8 h of dark at 28℃. For soil growth, germinated seeds were transferred to a mix of vermiculite: organic substrate (1:3) and cultured at 28℃ in chambers.

The Arabidopsis T-DNA insertion mutants were obtained from Arabidopsis Biological Resource Center and Fuzhou Aerosa Biotechnology. Seeds were sown onto soil, stratified at 4°C for 3 days, and grown in chambers under constant light or 16 h light/8 h dark and 70% relative humidity.

Maize cultivar B104 was used for this study. Seeds were placed on wet paper towels in the dark overnight at room temperature to break dormancy before being sown in soil for germination. Plants were grown under 22°C with continuous light for chilling assays or under 26°C with continuous light for stomatal measurements.

Plasmid construction and plant transformation

Specific targets for guide RNA spacer sequences were designed for CRISPR (Clustered regularly interspaced short palindromic repeats)/Cas9 constructs by using the CRISPR-PLANT website (http://www.genome.arizona.edu/crispr/CRISPR). Two guide RNA targets were cloned into the PHUE411 vector[55], and the resulting construct was transformed into Nip through *Agrobacterium tumefaciens*-mediated transformation[56]. For overexpression constructs, the coding sequence (CDS) was amplified and cloned into the pCAMBIA1300-GFP vector (Addgene). For GST (Glutathione s transferase) fusion constructs, the CDS was cloned into pGEX-2T vectors (Addgene) using a homologous recombination system (Vazyme, China). For His-fusion constructs, the CDS was cloned into the pET-30a vector. For Myc-fusion constructs, the CDS was cloned into pCAMBIA1300-221 vectors (Addgene). Vector details are listed in Supplementary Table 3. Transgenic plants were selected by hygromycin.Primes details are listed in Supplementary Table 2.

The *Zmctk1* mutants were generated in maize using methods as described previously[54,55]. Agrobacterium-mediated genetic transformation was performed by the Crop Bioengineering Laboratory at the Iowa State University.

Chilling tolerance assays

Chilling tolerance and ion leakage assays for rice plants were carried out using the method described previously[35].

For maize plants, chilling growth assay was done on seedlings grown at 26°C till 3-leaf stage. Plants were subsequently grown at 10°C for three weeks before they were transferred to 26°C for recovery for two weeks.

For freezing tolerance assay in Arabidopsis, plants were germinated and grown at 22°C for two weeks. They were then subjected to -8°C for 5 h before being returned to 22°C for one week's recovery. Plants were covered with humidity dome the first at the recovery.

Stomata related assays

Epidermal impressions were made using clear nail polish[63]. Dried nail polish was peeled from leaf epidermis and epidermal impression was observed under an Olympus BX53 microscope. Stomatal width and length were measured on the images using ImageJ software. Sixty stomata from four leaves were measured for each sample.

Transpiration rate was measured using a steady-state porometer (METER SC-1). The second fully expanded leaf of the three-leaf stage plant was placed and stabilized within the chamber of the porometer for 30 s. Measurements were taken on the middle section of leaf. Data were collected from six leaves per genotype and time point.

Leaf water loss was measured by fresh weight from ten uniformly grown seedlings per replicate, with three replicates in total to minimize individual variation. Water loss rate was expressed as the percentage of weight difference divided by the initial fresh weight.

For leaf surface temperature, thermal images were captured using a thermal imager (FOTRIC 225S). Quantification of temperature was performed using AnalyzIR (FOTRIC TOOLS).

RNA extraction and RT-qPCR

One microgram of total RNA was reverse transcribed into cDNA using HiScript II RT SuperMix (Vazyme). *OsActin* (*LOC_Os03g50885*) was used as the reference gene. Expression levels were determined using the comparative cycle threshold method (Vazyme). Primers used for RT-qPCR for each gene are detailed in Supplementary Table 2.

RNA-Seq and data analysis

Total RNA was isolated from the leaves of 14-day-old rice plants using Trizol reagent (TsingZol). Library construction and deep sequencing were performed by the Nanjing Jiangbei New Area Biopharmaceutical Public Service Platform Company Limited using the Illumina NovaSeq 6000 platform. DEGs were identified by DESeq2[56], with adjusted *P*-values set at $p<0.05$ and a Fold Change>2.

Protein extraction and immunoblotting

Plant tissues were ground into powder using liquid nitrogen, and extracted by protein extract buffer (50 mM HEPES (pH 7.5), 75 mM NaCl, 1 mM EGTA, 1 mM $MgCl_2$, 1 mM NaF, 10% glycerol, Complete^{TM} EDTA-free protease inhibitor and PhosSTOP^{TM} phosphatase inhibitor cocktails) at 500 µL of per 0.3 g of fresh tissue. Supernatants were collected following centrifugation at 13000 g for 15 min at 4°C as the protein extracts.

Proteins were separated by SDS-PAGE on 12% gels. Proteins were transferred to polyvinylidene difluoride (PVDF) membranes (GE Healthcare) in a wet tank unit (Bio-Rad). Membranes were incubated with primary anti-RPS6 antibody (rice: Solarbio, China, maize and Arabidopsis: Agrisera, Sweden) diluted to 1:1000, and polyclonal primary anti-RPS6A-P240 phosphorylated (Ser240) antibody diluted to 1:1000 (rice: Solarbio, maize and Arabidopsis: Agrisera). Antibodies were diluted in TBS-T (Tris-buffered saline with tween-20) containing 1% w/v BSA and incubated overnight at 4°C. Following six washing steps in TBS-T, membranes were incubated with a horseradish peroxidase conjugated goat anti-rabbit IgG secondary antibody (Santa Cruz Biotechnology) diluted 1:5000 in TBS-T containing 1% w/v BSA for 2 h.

After three washing steps in TBS-T, proteins were detected by incubating the membranes in Clarity Western ECL substrate (Bio-Rad). The band intensities were quantified using ImageJ software.

In vitro phosphoproteomic analysis

In vitro phosphoproteomics was carried out using the method described previously[57]. Briefly, Total proteins extracted from chilling treated plants were dephosphorylated and then incubated with recombinant OsCTK1 in a kinase reaction containing 1 mM γ-[$^{18}O_4$] ATP. Peptides labelled with ^{18}O were identified by Mass Spec.

Liquid chromatography tandem mass spectrometry analysis

The GFP fusion protein was purified using the GFP-trap IP (KT Life). The bound proteins were eluted from the beads by heating at 95℃ for 10 min. Proteins were fractionated on 12% SDS-PAGE (Bio-Rad) and stained with Coomassie brilliant blue. Bands were excised and cut into small pieces and subjected to MS analyses (BGI).

Co-immunoprecipitation assay

Co-IP assay was carried out as described previously[35].

Isolation and transformation of rice protoplasts

Protoplast isolation was done using method previously described[58]. Specifically, 5 grams rice leaf strips of 0.5 mm size were digested in 10 mL enzyme solution (1.5% cellulose R10, 0.75% macerozyme R10, 0.6 M mannitol, 10 mM MES) for 6 h in dark with gentle shaking (40 rpm) at 28℃. PEG-mediated transfections were carried out as described[59]. Specifically, 5-10 µg of plasmid DNA were mixed with 100 µL protoplasts.

Phos-tag mobility shift assay

Phos-tag reagent (AAL-107, Wako) was used for the phosphoprotein mobility-shift assay as described[60]. Protein extracts were separated on 12% (w/v) SDS-PAGE gel containing 50 µM Phos-tag and 100 µM $MnCl_2$.

Cell-free protein degradation assay

Cell-free protein degradation assay was performed as described[61] with minor modifications. Total proteins were extracted from 14-days seedlings. Total proteins (0.3 g leaf to 500 µL extraction buffer) were incubated with purified recombinant proteins (5 mg) and 10 mM ATP. Proteins were detected with anti-His monoclonal antibody (Sangon Biotech). The Rubisco large (RbcL) subunit, detected by Ponceau S staining, was used as a loading control.

Cell fractionation assay

Soluble and nuclear proteins were isolated using Plant Nuclei Isolation/Extraction Kit (Sigma). PEPC protein was used as a cytosolic marker, and histone H3 was used as a nuclear marker.

Declarations

Acknowledgements

We thank Professor Chengqiang Ding for the *Ossnrk1a* mutant seeds as well as Dr. Jing Li and Bioinformatics Center at Nanjing Agricultural University for RNA-seq analysis.

Author contributions

J.H. and B.Z. supervised the study. J.W., H.M., P.V., Y.Z., J.Y., G.X., R.Y., S.L. and S.Lu. performed the experiments, among them, J.W., B.Z. and H.M. drafted the manuscript. J.H. revised the manuscript. All authors contributed to the discussion and approved the final manuscript.

Funding

This study was supported by United States Department of Agriculture NIFA (2022-67013-37040), the Natural Science Foundation of China (32441064, 31971827, 32370309), Jiangsu Agricultural Science and Technology Innovation Fund (CX (23)1033) and China Postdoctoral Science Foundation (2024M761438, GZC20252664).

Competing interests

The authors declare no competing interests.

References

1. Ding, Y. L., Shi, Y. T. & Yang, S. H. Regulatory Networks Underlying Plant Responses and Adaptation to Cold Stress. *Annu Rev Genet* **58**, 43-65, doi:10.1146/annurev-genet-111523-102226 (2024).
2. Kidokoro, S., Shinozaki, K. & Yamaguchi-Shinozaki, K. Transcriptional regulatory network of plant cold-stress responses. *Trends in Plant Science* **27**, 922-935, doi:10.1016/j.tplants.2022.01.008 (2022).
3. Zhu, J. K. Abiotic Stress Signaling and Responses in Plants. *Cell* **167**, 313-324, doi:10.1016/j.cell.2016.08.029 (2016).
4. Jia, M. R. *et al.* Chilling-induced phosphorylation of IPA1 by OsSAPK6 activates chilling tolerance responses in rice. *Cell Discov* **8**, doi:ARTN 71, 10.1038/s41421-022-00413-2 (2022).
5. Xu, Y. F., Wang, R. C., Wang, Y. M., Zhang, L. & Yao, S. G. A point mutation in LTT1 enhances cold tolerance at the booting stage in rice. *Plant Cell Environ* **43**, 992-1007, doi:10.1111/pce.13717

(2020).

6. Hua, J. Defining roles of tandemly arrayed CBF genes in freezing tolerance with new genome editing tools. *New Phytol* **212**, 301-302, doi:10.1111/nph.14183 (2016).
7. Shi, Y., Ding, Y. & Yang, S. Molecular Regulation of CBF Signaling in Cold Acclimation. *Trends Plant Sci* **23**, 623-637, doi:10.1016/j.tplants.2018.04.002 (2018).
8. Jia, Y. X. *et al.* The triple mutants reveal the essential functions of in cold acclimation and allow the definition of CBF regulons in. *New Phytol* **212**, 345-353, doi:10.1111/nph.14088 (2016).
9. Jiang, H. *et al.* Natural polymorphism of ZmICE1 contributes to amino acid metabolism that impacts cold tolerance in maize. *Nat Plants* **8**, 1176-1190, doi:10.1038/s41477-022-01254-3 (2022).
10. Wang, H. *et al.* Dehydration-Responsive Element Binding Protein 1C, 1E, and 1G Promote Stress Tolerance to Chilling, Heat, Drought, and Salt in Rice. *Front Plant Sci* **13**, 851731, doi:10.3389/fpls.2022.851731 (2022).
11. Kishor, P. B. K. *et al.* Regulation of proline biosynthesis, degradation, uptake and transport in higher plants: Its implications in plant growth and abiotic stress tolerance. *Curr Sci India* **88**, 424-438 (2005).
12. Bonnecarrere, V. *et al.* Response to photoxidative stress induced by cold in japonica rice is genotype dependent. *Plant Sci* **180**, 726-732, doi:10.1016/j.plantsci.2011.01.023 (2011).
13. Zhang, J. B., Chen, X. X., Song, Y. J. & Gong, Z. Z. Integrative regulatory mechanisms of stomatal movements under changing climate. *J Integr Plant Biol* **66**, 368-393, doi:10.1111/jipb.13611 (2024).
14. Agurla, S., Gahir, S., Munemasa, S., Murata, Y. & Raghavendra, A. S. Mechanism of Stomatal Closure in Plants Exposed to Drought and Cold Stress. *Adv Exp Med Biol* **1081**, 215-232, doi:10.1007/978-981-13-1244-1_12 (2018).
15. Honour, S. J., Webb, A. A. R. & Mansfield, T. A. The Responses of Stomata to Abscisic-Acid and Temperature Are Interrelated. *P Roy Soc B-Biol Sci* **259**, 301-306, doi:DOI 10.1098/rspb.1995.0044 (1995).
16. Sun, C. Y. *et al.* PKS5 Confers Cold Tolerance by Controlling Stomatal Movement and Regulating Cold-Responsive Genes in Arabidopsis. *Life-Basel* **12**, doi:ARTN 1633, 10.3390/life12101633 (2022).
17. Wilkinson, S., Clephan, A. L. & Davies, W. J. Rapid low temperature-induced stomatal closure occurs in cold-tolerant leaves but not in cold-sensitive tobacco leaves, via a mechanism that involves apoplastic calcium but not abscisic acid. *Plant Physiol* **126**, 1566-1578, doi:DOI 10.1104/pp.126.4.1566 (2001).
18. Lv, J. *et al.* Reciprocal regulation between the negative regulator PP2CG1 phosphatase and the positive regulator OST1 kinase confers cold response in. *J Integr Plant Biol* **63**, 1568-1587, doi:10.1111/jipb.13100 (2021).
19. Liu, Z. Y. *et al.* Phytocytokine signalling reopens stomata in plant immunity and water loss. *Nature* **605**, 332-+, doi:10.1038/s41586-022-04684-3 (2022).

20. Wang, K. *et al.* EAR1 Negatively Regulates ABA Signaling by Enhancing 2C Protein Phosphatase Activity. *Plant Cell* **30**, 815-834, doi:10.1105/tpc.17.00875 (2018).
21. Luo, L. L. *et al.* Tolerance to multiple abiotic stresses is mediated by interacting CNGC proteins that regulate Ca^{2+} influx and stomatal movement in rice. *J Integr Plant Biol* **67**, 226-242, doi:10.1111/jipb.13829 (2025).
22. Zhang, H., Zhao, Y. & Zhu, J. K. Thriving under Stress: How Plants Balance Growth and the Stress Response. *Developmental Cell* **55**, 529-543, doi:10.1016/j.devcel.2020.10.012 (2020).
23. Baena-González, E., Rolland, F., Thevelein, J. M. & Sheen, J. A central integrator of transcription networks in plant stress and energy signalling. *Nature* **448**, 938-U910, doi:10.1038/nature06069 (2007).
24. Baena-González, E. & Hanson, J. Shaping plant development through the SnRK1-TOR metabolic regulators. *Curr Opin Plant Biol* **35**, 152-157, doi:10.1016/j.pbi.2016.12.004 (2017).
25. Hulsmans, S., Rodriguez, M., De Coninck, B. & Rolland, F. The SnRK1 Energy Sensor in Plant Biotic Interactions. *Trends in Plant Science* **21**, 648-661, doi:10.1016/j.tplants.2016.04.008 (2016).
26. Wurzinger, B., Nukarinen, E., Nägele, T., Weckwerth, W. & Teige, M. The SnRK1 Kinase as Central Mediator of Energy Signaling between Different Organelles. *Plant Physiol* **176**, 1085-1094, doi:10.1104/pp.17.01404 (2018).
27. Broeckx, T., Hulsmans, S. & Rolland, F. The plant energy sensor: evolutionary conservation and divergence of SnRK1 structure, regulation, and function. *Journal of Experimental Botany* **67**, 6215-6252, doi:10.1093/jxb/erw416 (2016).
28. Tsai, A. Y. L. & Gazzarrini, S. Trehalose-6-phosphate and SnRK1 kinases in plant development and signaling: the emerging picture. *Front Plant Sci* **5**, doi:ARTN 119, 10.3389/fpls.2014.00119 (2014).
29. Emanuelle, S., Doblin, M. S., Stapleton, D. I., Bacic, A. & Gooley, P. R. Molecular Insights into the Enigmatic Metabolic Regulator, SnRK1. *Trends in Plant Science* **21**, 341-353, doi:10.1016/j.tplants.2015.11.001 (2016).
30. Martínez-Barajas, E. & Coello, P. Review: How do SnRK1 protein kinases truly work? *Plant Sci* **291**, doi:ARTN 110330, 10.1016/j.plantsci.2019.110330 (2020).
31. Ramon, M. *et al.* Default Activation and Nuclear Translocation of the Plant Cellular Energy Sensor SnRK1 Regulate Metabolic Stress Responses and Development. *Plant Cell* **31**, 1614-1632, doi:10.1105/tpc.18.00500 (2019).
32. Mair, A. *et al.* SnRK1-triggered switch of bZIP63 dimerization mediates the low-energy response in plants. *Elife* **4**, doi:ARTN e05828, 10.7554/eLife.05828 (2015).
33. Dietrich, K. *et al.* Heterodimers of the Transcription Factors bZIP1 and bZIP53 Reprogram Amino Acid Metabolism during Low Energy Stress. *Plant Cell* **23**, 381-395, doi:10.1105/tpc.110.075390 (2011).
34. Wang, W. T. *et al.* SnRK1 stimulates the histone H3K27me3 demethylase JMJ705 to regulate a transcriptional switch to control energy homeostasis. *Plant Cell* **33**, 3721-3742, doi:10.1093/plcell/koab224 (2021).

35. Wu, J. *et al.* A major gene for chilling tolerance variation in Indica rice codes for a kinase OsCTK1 that phosphorylates multiple substrates under cold. *New Phytol*, doi:10.1111/nph.19696 (2024).
36. Qu, L., Liu, M., Zheng, L., Wang, X. & Xue, H. Data-independent acquisition-based global phosphoproteomics reveal the diverse roles of casein kinase 1 in plant development. *Sci Bull (Beijing)* **68**, 2077-2093, doi:10.1016/j.scib.2023.08.017 (2023).
37. Knippschild, U. *et al.* The casein kinase I family:: participation in multiple cellular processes in eukaryotes. *Cell Signal* **17**, 675-689, doi:10.1016/j.cellsig.2004.12.011 (2005).
38. Dai, C. & Xue, H. W. Rice early flowering1, a CKI, phosphorylates DELLA protein SLR1 to negatively regulate gibberellin signalling. *EMBO J* **29**, 1916-1927, doi:10.1038/emboj.2010.75 (2010).
39. Tan, S. T., Dai, C., Liu, H. T. & Xue, H. W. Arabidopsis casein kinase1 proteins CK1.3 and CK1.4 phosphorylate cryptochrome2 to regulate blue light signaling. *Plant Cell* **25**, 2618-2632, doi:10.1105/tpc.113.114322 (2013).
40. Tan, S. T. & Xue, H. W. Casein kinase 1 regulates ethylene synthesis by phosphorylating and promoting the turnover of ACS5. *Cell Rep* **9**, 1692-1702, doi:10.1016/j.celrep.2014.10.047 (2014).
41. Shi, W. *et al.* Hydrogen peroxide is required for light-induced stomatal opening across different plant species. *Nature Communications* **15**, doi:ARTN 5081, 10.1038/s41467-024-49377-9 (2024).
42. Hu, Y. X. *et al.* Sucrose nonfermenting-1-related protein kinase 1 regulates sheath-to-panicle transport of nonstructural carbohydrates during rice grain filling. *Plant Physiol* **189**, 1694-1714, doi:10.1093/plphys/kiac124 (2022).
43. Hey, S., Mayerhofer, H., Halford, N. G. & Dickinson, J. R. DNA sequences from arabidopsis, which encode protein kinases and function as upstream regulators of Snf1 in yeast. *J Biol Chem* **282**, 10472-10479, doi:10.1074/jbc.M611244200 (2007).
44. Shen, W., Reyes, M. I. & Hanley-Bowdoin, L. Arabidopsis Protein Kinases GRIK1 and GRIK2 Specifically Activate SnRK1 by Phosphorylating Its Activation Loop. *Plant Physiol* **150**, 996-1005, doi:10.1104/pp.108.132787 (2009).
45. Martin-StPaul, N., Delzon, S. & Cochard, H. Plant resistance to drought depends on timely stomatal closure. *Ecol Lett* **20**, 1437-1447, doi:10.1111/ele.12851 (2017).
46. Ramachandra Reddy, A., Chaitanya, K. V. & Vivekanandan, M. Drought-induced responses of photosynthesis and antioxidant metabolism in higher plants. *J Plant Physiol* **161**, 1189-1202, doi:10.1016/j.jplph.2004.01.013 (2004).
47. Baena-Gonzalez, E. & Sheen, J. Convergent energy and stress signaling. *Trends Plant Sci* **13**, 474-482, doi:10.1016/j.tplants.2008.06.006 (2008).
48. Wilson, D. F. Contribution of diffusion to the oxygen dependence of energy metabolism in cells. *Experientia* **46**, 1160-1162, doi:10.1007/BF01936927 (1990).
49. Cho, H. Y., Wen, T. N., Wang, Y. T. & Shih, M. C. Quantitative phosphoproteomics of protein kinase SnRK1 regulated protein phosphorylation in Arabidopsis under submergence. *J Exp Bot* **67**, 2745-2760, doi:10.1093/jxb/erw107 (2016).

50. Bita, C. E. & Gerats, T. Plant tolerance to high temperature in a changing environment: scientific fundamentals and production of heat stress-tolerant crops. *Front Plant Sci* **4**, doi:ARTN 273, 10.3389/fpls.2013.00273 (2013).
51. Li, J. G. *et al.* Brassinosteroid and Hydrogen Peroxide Interdependently Induce Stomatal Opening by Promoting Guard Cell Starch Degradation. *Plant Cell* **32**, 984-999, doi:10.1105/tpc.19.00587 (2020).
52. Flütsch, S. *et al.* Guard Cell Starch Degradation Yields Glucose for Rapid Stomatal Opening in Arabidopsis. *Plant Cell* **32**, 2325-2344, doi:10.1105/tpc.18.00802 (2020).
53. Huang, X. Y. *et al.* A previously unknown zinc finger protein, DST, regulates drought and salt tolerance in rice via stomatal aperture control. *Genes Dev* **23**, 1805-1817, doi:10.1101/gad.1812409 (2009).
54. Xing, H. L. *et al.* A CRISPR/Cas9 toolkit for multiplex genome editing in plants. *BMC Plant Biol* **14**, 327, doi:10.1186/s12870-014-0327-y (2014).
55. Nishimura, A., Aichi, I. & Matsuoka, M. A protocol for Agrobacterium-mediated transformation in rice. *Nature Protocols* **1**, 2796-2802, doi:10.1038/nprot.2006.469 (2006).
56. Love, M. I., Huber, W. & Anders, S. Moderated estimation of fold change and dispersion for RNA-seq data with DESeq2. *Genome Biol* **15**, doi:ARTN 550, 10.1186/s13059-014-0550-8 (2014).
57. Wang, P. C. *et al.* Mapping proteome-wide targets of protein kinases in plant stress responses. *P Natl Acad Sci USA* **117**, 3270-3280, doi:10.1073/pnas.1919901117 (2020).
58. Zhang, Y. *et al.* A highly efficient rice green tissue protoplast system for transient gene expression and studying light/chloroplast-related processes. *Plant Methods* **7**, doi:Artn 30, 10.1186/1746-4811-7-30 (2011).
59. Yoo, S. D., Cho, Y. H. & Sheen, J. mesophyll protoplasts:: a versatile cell system for transient gene expression analysis. *Nature Protocols* **2**, 1565-1572, doi:10.1038/nprot.2007.199 (2007).
60. Mao, G. H. *et al.* Phosphorylation of a WRKY Transcription Factor by Two Pathogen-Responsive MAPKs Drives Phytoalexin Biosynthesis in. *Plant Cell* **23**, 1639-1653, doi:10.1105/tpc.111.084996 (2011).
61. Ding, Y. L. *et al.* OST1 Kinase Modulates Freezing Tolerance by Enhancing ICE1 Stability in. *Developmental Cell* **32**, 278-289, doi:10.1016/j.devcel.2014.12.023 (2015).
62. Li, R. Q. et al. OsNAC5 orchestrates OsABI5 to fine-tune cold tolerance in rice. *J Integr Plant Biol* **66**, 660-682, doi:10.1111/jipb.13585 (2024).
63. Wu, S. and Zhao, B. Using clear nail polish to make Arabidopsis epidermal impressions for measuring the change of stomatal aperture size in immune response. *Methods Mol. Biol* **1578**, 243-248, doi: 10.1007/978-1-4939-6859-6_20 (2017).

Figures

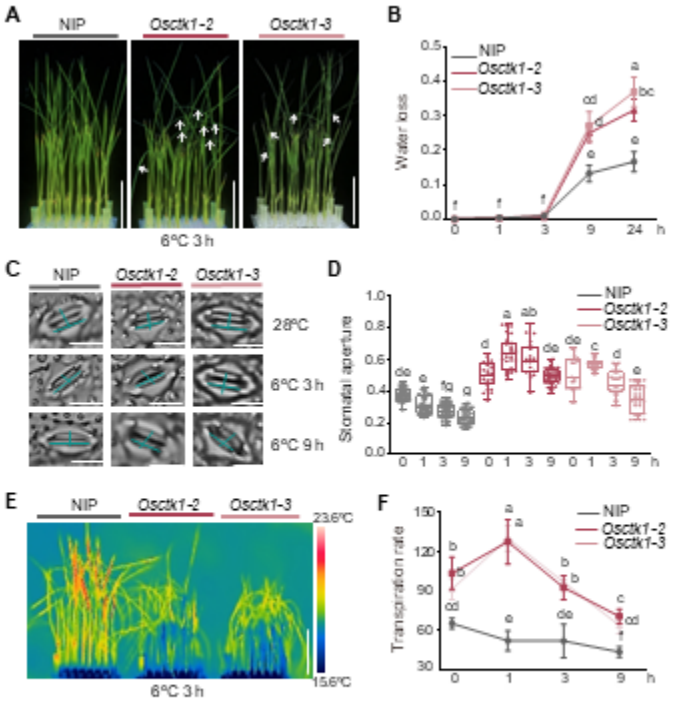


Fig.1: *OsCTK1* promotes stomatal closure under chilling.

Figure 1

OsCTK1 promotes stomatal closure under chilling.

(A) Chilling induced leaf drooping in wild-type Nipponbare (NIP), *Osctk1-2* and *Osctk1-3* at 3 h of 6°C treatments. All drooped leaves are indicated by white arrows, and bars are 5 cm, (B) Water loss (shown as percentage of fresh weight loss after chilling compared to initial weight) in leaves in NIP, *Osctk1-2* and *Osctk1-3*. (C-D) Stomatal phenotypes (C) and quantification of stomatal aperture (D) of NIP, *Osctk1-2* and *Osctk1-3* mutants before (0 h) and after a 6°C treatment. Stomatal aperture is defined as the ratio of width and length (indicated by lines in cyan in C) of the stomata. Dot plots in C are from 60 stomata per genotype time point. Bars in C represent 100 μm. (E) Leaf surface temperature shown by the infrared thermal images of NIP, *Osctk1-2* and *Osctk1-3* at 3 h of 6°C treatment (F) Transpiration rate (mmol H_2O m^{-2} s^{-1}) of NIP, *Osctk1-2* and *Osctk1-3* before (0 h) and after the 6°C treatments. Shown are means and standard deviations from 60 stomata. Letters indicate significant differences at $p< 0.05$ by Duncan's multiple range test among the means via ANOVA in B, D and F.

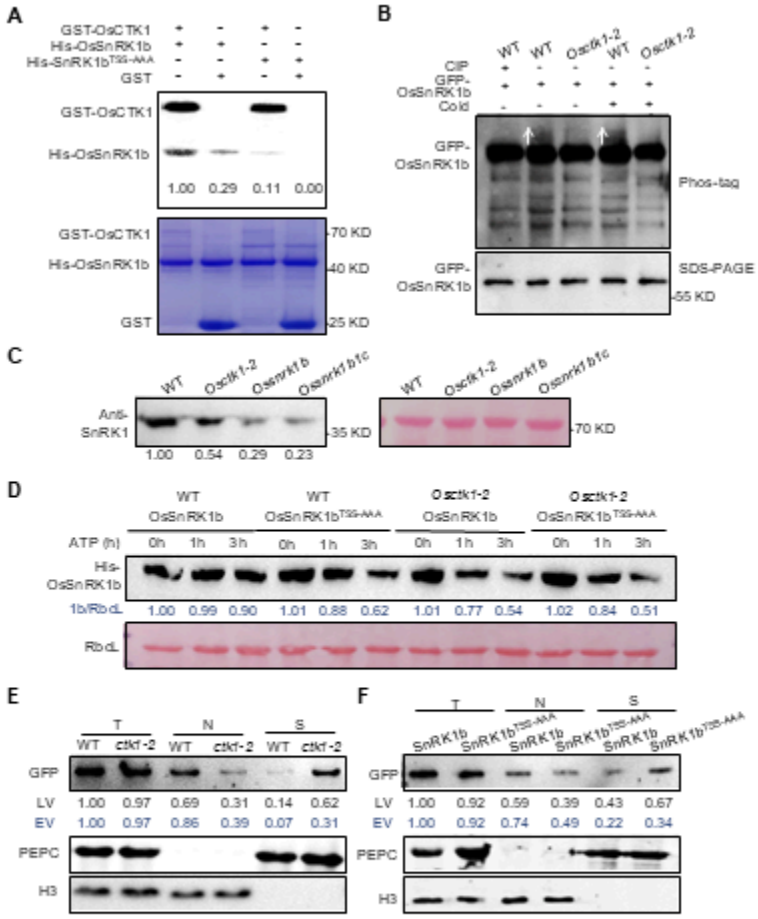


Fig.2: OsCTK1 phosphorylates and stabilizes OsSnRK1b.

Figure 2

OsCTK1 phosphorylates and stabilizes OsSnRK1b.

(A) Phosphorylation of OsSnRK1b by OsCTK1. Shown are autoradiograph (top panel) and Coomassie Brilliant Blue (CBB) staining (bottom panel) of proteins from the kinase reaction consisting of recombinant OsCTK1 and OsSnRK1b (wild-type NIP form or the mutant form and OsSnRK1b$^{TSS-AAA}$separated on a 12% SDS-PAGE gel. Relative phosphorylation levels of OsSnRK1b (shown as black numbers) are quantified with the level of OsSnRK1b by OsCTK1 set as 1. (B) Phosphorylation of GFP-OsSnRK1b in plants carrying GFP-OsSnRK1b transgene in the NIP or *Osctk1-2* background with or without 30 min of chilling (6°C) treatment. Total proteins were separated on the phos-tag gel (top panel) and SDS-PAGE gel (bottom panel). CIP samples were treated with calf intestine phosphatase at 37°C for 30 min. (C) Immunoblot of total proteins of NIP, *Osctk1-2*, *Ossnrk1b-3* and *Ossnrk1b1c* detected by an anti-SnRK1b antibody. RbcL protein (Ponceau S stained) was used as the loading control of total protein. Numbers are relative amount of OsSnRK1b compared to the NIP. (D) Immunoblot of recombinant His-tagged OsSnRK1b and OsSnRK1b$^{TSS-AAA}$ proteins after incubation at 28°C with total protein extracts

from wild-type NIP or *Osctk1-2* mutant plants in the presence of ATP for 0 h, 1 h or 3 h. RbcL protein stained with Ponseu S was used as the loading control of total proteins. The numbers are relative abundance of His-OsSnRK1b normalized to that of His-OsSnRK1b with WT extract at 0 h. (E) Immunoblot of GFP-OsSnRK1b in total protein extracts, nuclear fraction and cytosol fraction from protoplasts of wild-type NIP or the *Osctk1-2* mutant transformed with GFP-OsSnRK1b. (F) Immunoblot of GFP-OsSnRK1b and GFP-OsSnRK1b$^{TSS\text{-}AAA}$ proteins in total protein extracts, nuclear fraction and cytosol fraction of wild-type NIP protoplasts transformed with the GFP fusion constructs. For (E) and (F), blots were probed with antibodies against GFP, PEPC (a cytosolic protein) and H3 (a nuclear protein) respectively. Loaded on the gels are 25% of the total proteins (T), 20% of nuclear proteins (N), and 50% of the cytoplasmic protein (S). LV (loading value): GFP signals quantified from blot with the first sample (WT T) set as 1. EV (equalized value): GFP signals adjusted with equalized loading of N, S and T with the first sample (WT T) set as 1.

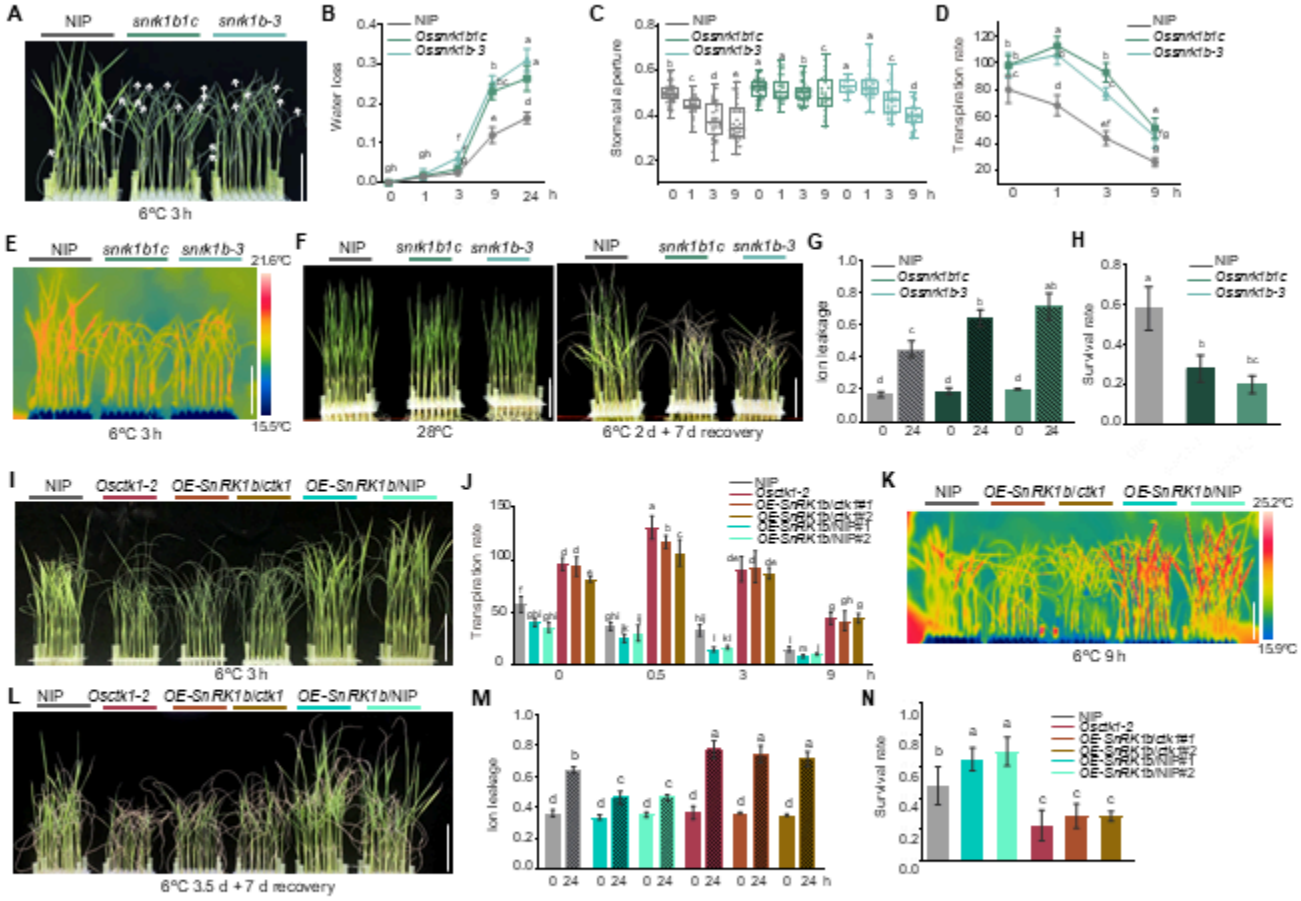


Fig.3: *OsSnRK1b* overexpression promotes stomatal closure and chilling tolerance in an *OsCTK1*-depdent manner.

Figure 3

OsSnRK1b overexpression promotes stomatal closure and chilling tolerance in an _OsCTK1_-depdent manner.

(A) Leaf drooping phenotypes in NIP and the *Ossnrk1b1c* and *Ossnrk1b-3* mutants under chilling. Shown are three-leaf-stage seedlings grown at 28℃ for two-weeks-old before (0 h) and after a 6℃ treatment for 3 h. All drooped leaves are indicated by white arrows. Bars are 5 cm. (B) Water loss in leaves in NIP, *Ossnrk1b1c* and *Ossnrk1b-3*. (C) Quantification of stomatal aperture of NIP, *Ossnrk1b1c* and *Ossnrk1b-3* mutants before (0 h) and after a 6℃ treatment. (D) Transpiration rate (mmol H_2O m^{-2} s^{-1}) of NIP, *Ossnrk1b1c* and *Ossnrk1b-3* before (0 h) and after 6℃ treatments. Shown are means and standard deviations from 60 stomata. (E) Leaf surface temperature shown by the infrared thermal images of NIP, *Ossnrk1b1c* and *Ossnrk1b-3* at 3 h of 6℃ treatments. (F-H) Plant morphology (F), ion leakage rates (G) and survival rates (H) of NIP, *Ossnrk1b1c* and *Ossnrk1b-3* plants of three-leaf stage before and after 6℃ chilling treatments. Plant morphology and survival rates were taken after of 6℃ treatment for 2 days followed by 7 days of recovery at 28℃. Bars are 5 cm in F. Ion leakage were measured at 0 h and 24 h of 6℃ treatments. (I-K) Leaf drooping (I), transpiration (J) and thermal imaging (K) of NIP, *Osctk1-2*, OE-*SnRK1b*/NIP (#2 and #3), and OE-*SnRK1b*/*ctk1* (#1 and #2) plants after 6℃ treatments as specified. White arrows in (I) indicate drooped leaves. Transpiration rate is mmol H_2O m^{-2} s^{-1}. A total of 60 stomata per genotype/time point were used for quantifications in (J). The bar in (I) is 5 cm. (L-N) Plant morphology (L), ion leakage rates (M) and survival rates (N) of NIP, *Ossnrk1b1c* and *Ossnrk1b-3* plants of three-leaf stage with 6℃ chilling treatments. Plant morphology and survival rates were taken after of 6℃ treatment for 3.5 days followed by 7 days of recovery at 28℃. Bars are 5 cm in L. Ion leakage were measured at 0 h and 24 h of 6℃ treatments. Letters indicate significant differences at $p< 0.05$ by Duncan's multiple range test among the means via ANOVA in B-D, G-H, J and M-N.

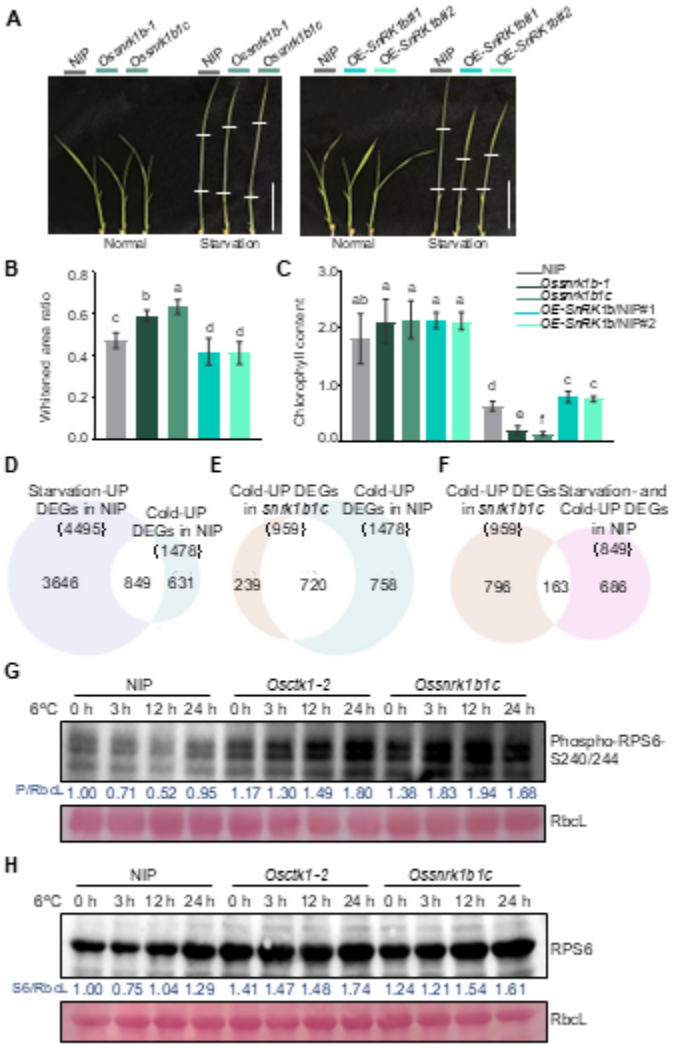


Fig.4: OsSnRK1b regulates starvation response

Figure 4

OsSnRK1b regulates starvation response.

(A) Starvation response phenotypes of NIP, *Ossnrk1b-1*, *Ossnrk1b1c*, and *OsSnRK1b* overexpression lines (OE-*SnRK1b*#1 and #2). Seedlings grown at 28℃ for 4 days followed by 7 days of growth under light (normal) or dark (starvation) before photographed. Bars are 5 cm. (B) Ratio of yellow leaf segment (flanked by white lines in A) versus total leaf length of seedlings in (A). (C) Chlorophyll content of above plants. Letters indicate significant differences at $p < 0.05$ by Duncan's multiple range test among the means via ANOVA in B-C. (D) Venn diagrams of starvation-induced up DEGs and 3 h cold-induced up DEGs in the NIP. (E) Venn diagram of 3 h cold-induced up DEGs in the NIP and the *Ossnrk1b1c* mutant. (F) Venn diagram of the cold-induced up DEGs in the *Ossnrk1b1c* mutant and starvation-induced and cold-induced up DEGs. (G) Immunoblot of Ser240/244 phosphorylation of RPS6 in NIP, *Ossnrk1b1c*and *Osctk1-2* without (0 h) and with 3 h, 12 h, and 24 h of 6°C chilling treatment. Ponseu S stained RbcL (bottom panel) was used as the loading control. Numbers indicate relative abundance of phosphorylated

RPS6 normalized to the first sample (NIP at 0 h). (H) Immunoblot of RPS6 protein in wild-type NIP, *Ossnrk1b1c* and *Osctk1-2* seedlings before (0 h) and 3 h to 24 h after 6°C chilling treatment. Bottom panel shows stained RbcL as loading control. Numbers indicate relative abundance of RPS6 normalized to the first sample (NIP at 0 h).

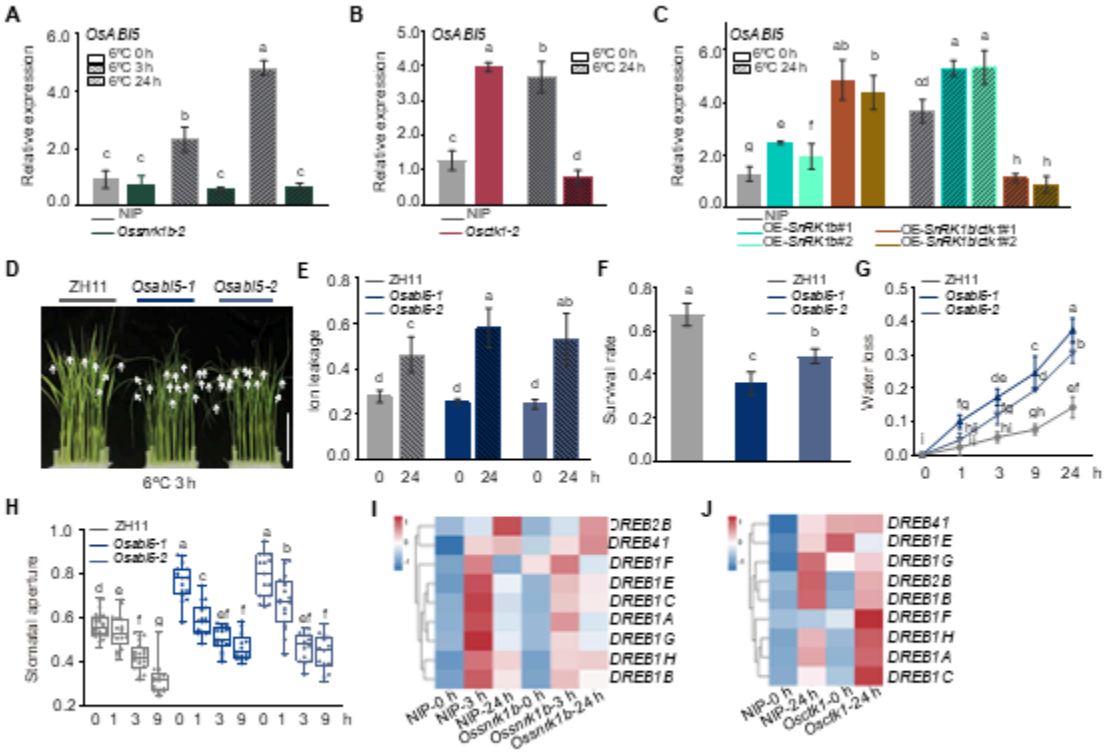


Fig.5: *OsABI5* positively regulates stomatal closure and chilling tolerance.

Figure 5

OsABI5 positively regulates stomatal closure and chilling tolerance.

(A-C) Expression of *OsABI5*at 0 h, 3 h or 24 h after chilling (6℃) treatment in wild type and *Ossnrk1b-2*(A), *Osctk1-2* (B) as well as OE-*SnRK1b*/NIP and OE-*SnRK1b*/*ctk1*lines (C) at three-leaf seedling stage. Shown are relative expression with *OsActin*as the reference gene as analyzed by qRT-PCR. (D) Leaf drooping phenotypes in wild-type ZH11, *Osabi5-1* and *Osabi5-2* seedlings under chilling. Shown are three-leaf-stage seedlings grown at 28℃ before (0 h) and after a 6℃ treatment for 3 h. Drooped leaves are indicated by white arrows. Bars are 5 cm. (E-F) Ion leakage rates (E) and survival rates (F) of ZH11, *Osabi5-1* and *Osabi5-2* plants of three-leaf stage before and after 6℃ chilling treatments. Survival rates were taken after of 6℃ treatment for 4 days followed by 7 days of recovery at 28℃. Ion leakage was measured at 0 h and 24 h of 6℃ treatments. (G) Water loss in leaves in ZH11, *Osabi5-1*and *Osabi5-2* plants before (0 h) and after a 6℃ treatment for 1 h, 3 h, 9 h and 24 h. (H) Quantification of stomatal aperture of ZH11, *Osabi5-1*and *Osabi5-2* mutants before (0 h) and after a 6℃ treatment for 1 h, 3 h and 9 h. Letters indicate significant differences at $p<0.05$ by Duncan's multiple range test among the means via

ANOVA in A-C and E-H. (I-J) Expression of *OsDREB* genes shown as heat map before (0 h) and after 6°C treatments (3 h or 24 h) in wild-type NIP and *Ossnrk1b1c*(I) or *Osctk1-2* (J).

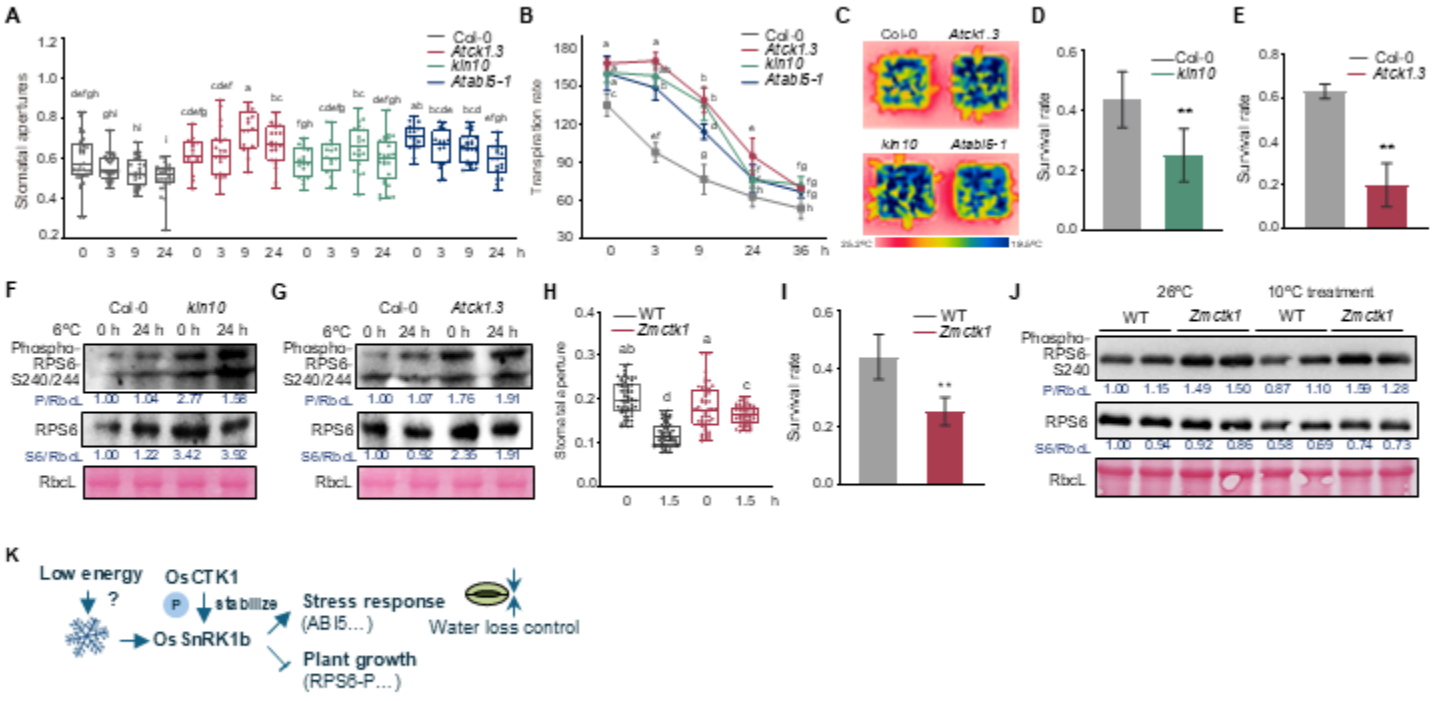


Fig.6: *CTK1*, *SnRK1* and *ABI5* in *Arabidopsis* and maize promote stomatal closure under chilling.

Figure 6

The *CTK1*, *SnRK1* and *ABI5* genes in Arabidopsis and maize promote stomatal closure under chilling stress.

(A) Dot plots of stomatal aperture (width/length) of wild type Col-0, *Atck1.3*, *kin10* and *Atabi5-1* before (0 h) and after treatment of 6°C for 3 h, 9 h and 24 h. (B) Quantification of transpiration rate (mmol H_2O m^{-2} s^{-1}) of wild type Col-0, *Atck1.3*, *kin10* and *Atabi5-1* leaves before (0 h) and after treatment of 6°C for 3 h, 9 h, 24 h and 36 h. Shown are means and standard deviations from 50 stomata for each genotype. Letters indicate significant differences at $p<0.05$ by Duncan's multiple range test among the means via ANOVA in A-B. (C) Infrared thermal images of wild type Col-0, *Atck1.3*, *kin10* and *Atabi5-1* leaves. (D-E) Survival rate of *kin10* (D) and *Atck1.3* (E) plants following 3 h of freezing treatment in Arabidopsis. Asterisk indicates statistical significance, with **$P< 0.01$, as determined by Student's *t*-test. (F-G) Immunoblots of Phospho-RPS6 and RPS6 levels in *kin10* (F) and *Atck1.3* (G) before (0 h) and after (24 h) 6°C treatment. RbcL stained by Ponseu S in the bottom panel serves as loading control. Numbers indicate relative abundance of RPS6 or phospho-RPS6 normalized to the first sample (Col-0 at 0 h). (H) Quantification of stomatal aperture (width/length) of wild type and *Zmctk1* before (0 h) and after a 6°C treatment for 1.5 h in maize. Letters indicate significant differences at $p< 0.05$ by Duncan's multiple range test among the means via ANOVA in H. (I) Survival rate analysis of wild type and *Zmctk1* following a 6°C treatment in

maize. Asterisk indicates statistical significance, with **P< 0.01, as determined by Student's t-test. (J) Immunoblots of Phospho-RPS6 and RPS6 levels in wild-type and *Zmctk1* (G) before (0 h) and after (24 h) 10°C treatment in maize. RbcL stained by Ponseu S in the bottom panel serves as loading control. Numbers indicate relative abundance of RPS6 or phospho-RPS6 normalized to the first sample (wild-type at 0 h). (K) Proposed model for OsCTK1 and OsSnRK1b mediated chilling tolerance. Under chilling stress, OsCTK1 phosphorylates and thereby stabilizes the low-energy sensor OsSnRK1b. This post-translational modification orchestrates bidirectional regulation of downstream pathways. On the one hand, activating the stress-responsive pathway centered on *OsABI5*, on the other hand, repressing growth-promoting pathways mediated by phosphorylated OsRPS6. Snowflakes represent chilling stress. P for phosphorylation. Arrowheads signify activation and T-bars represent inhibition.

Supplementary Files

This is a list of supplementary files associated with this preprint. Click to download.

- SupplementTableCTK1SnRK10820.xlsx
- SupplementfigureCTK1SnRK108232025.pdf